Chitosan-based melatonin bilayer coating for maintaining quality of fresh-cut products

Hangyue Zhao[a] (zhy-156@163.com, ORCID: 0000-0003-0179-1484)
Lei Wang[a] (wangley@zju.edu.cn, 0000-0002-6949-4489)
Tarun Belwal[a] (tarungbpihed@gmail.com, ORCID: 0000-0003-0434-1956)
Yunhong Jiang[b] (yunhongjiang@yahoo.com, ORCID: 0000-0003-3292-8164)
Dong Li[a] (dong_li@zju.edu.cn, ORCID: 0000-0002-1800-1656)
Yanqun Xu[a] (xuyanqun@zju.edu.cn, ORCID: 0000-0003-3488-9445)
Zisheng Luo[a,c] (luozisheng@zju.edu.cn, ORCID: 0000-0001-8232-9739)
Li Li[a,c,*] (lili1984@zju.edu.cn, ORCID: 0000-0002-1242-3866)

[a]Key Laboratory for Agro-Products Postharvest Handling of Ministry of Agriculture and Rural Affairs, College of Biosystems Engineering and Food Science, Zhejiang University, Hangzhou 310058, China
[b]Bristol Dental School, University of Bristol, Bristol BS1 2LY, UK
[c]Ningbo Research Institute, Zhejiang University, Ningbo 315100, China

*To whom correspondence should be addressed: Dr. Li Li (lili1984@zju.edu.cn; Telephone: +86-571-88981885; Fax: +86-571-88981885.)

Abstract

This work was designed to develop the chitosan-based melatonin layer-by-layer assembly (CMLLA) via the inclusion method and further to test the effectiveness on fresh produce. The structural characterizations and interaction present in CMLLA were investigated by the scanning electron microscope (SEM), X-ray diffraction (XRD) and Fourier Transform-Infrared spectroscopy (FTIR). The ratio of chitosan (CH) to carboxymethylcellulose (CMC) greatly influenced the mechanical properties, including the tensile strength, moisture content and color performance. The antioxidant capacity of CMLLA was determined by evaluating the scavenging effect and the antimicrobial activity was evaluated using the zone of inhibition against infected bacterial. Results showed that both antioxidant and antimicrobial properties of CMLLA were enhanced with the addition of melatonin (MLT). Furthermore, the possible practical application of CMLLA as edible coating on fresh products by was investigated. It was demonstrated that the CMLLA with 1.2% (w/v) CH, 0.8% (w/v) CMC and 50 mg/L MLT better contributed to the delay of chlorophyll degradation and the maintenance of shelf-life quality. Results from this study might open up new insights into the approaches of quality improvement of postharvest fresh products by incorporating the natural antioxidant compounds into natural polymers.

Keywords:

Melatonin-loaded; assembly; layer by layer; structural property; antioxidant capacity, antimicrobial activity

1. Introduction

The natural polysaccharides applied on packaging of fresh produces have increased tremendously with more emphases on development of eco-packaging coating materials in last few years (de Moraes Crizel et al., 2018; Medina-Jaramillo, Ochoa-Yepes, Bernal, & Famá, 2017). The incorporated natural bioactive compounds in packaging films are of great importance, which provides various functional properties to the films, such as antioxidant, antimicrobial. The advantages of selecting natural compounds over synthetic have well been reviewed and discussed over many years (Noronha, de Carvalho, Lino, & Barreto, 2014; Sozer & Kokini, 2009; Song et al., 2018). For instance, the higher toxicity of synthetic antioxidants was well explained and thus substituted by the natural antioxidants (Noronha, de Carvalho, Lino, & Barreto, 2014; Huang et al., 2015; Park, Choi, Hu, & Lee, 2013; Tang et al., 2016).

Among various natural antioxidants, melatonin (MLT), a natural hormone that is primarily released by the pineal gland to the blood circulation, exerts various biological activities such as antioxidant, antimicrobial, and anti-apoptotic (Wang et al., 2018; Arnao and Hernandez-Ruiz, 2018). In a recent study, MLT has been applied in preharvest and postharvest fresh products due to the excellent antioxidant capacity (Sun et al., 2019; Tan et al., 2007; Shi et al., 2015). For instance, Tan et al. (2007) reported that the improved antioxidant capacity and tolerance to copper contamination in pea plants by exogenous MLT (Tan et al., 2007). Moreover, MLT has been widely used to postpone chlorophyll degradation of barley leaves (Arnao & Hernández-Ruiz, 2009), and to reduce oxidative damage of grape cuttings (Meng et al., 2014). Considering the post-harvested products, the application of MLT could effectively prolong the shelf-life and also maintain the postharvest quality attributes (Tan et al., 2012; Liu et al., 2016). Furthermore, it was demonstrated that exogenous MLT significantly reduced the weight loss and decay incidence, as well as maintained firmness and total soluble solids of postharvest peach (Gao et al., 2016). In a recent report, the application of MLT was found to be effectively attenuate the fungal decay and maintain the nutritional quality of post-harvested strawberry as well as trigger the accumulation of H_2O_2 accumulation, which resulted from higher superoxide dismutase (SOD) activity (Aghdam et al., 2017). Overall, MLT potentially contributed to maintaining quality in postharvest fresh-cut products. However, the direct dose of MLT posed difficulties during the processing procedure as the low solubility of MLT in water, while the antioxidant capacity of MLT was significantly affected. Thus, the suitable delivery system loading MLT are essential to sustain and prolong its efficiency, which is analogous to that used in drug and medical industry (Malafaya, Silva, & Reis, 2007). Chitosan, a poly-*N*-acetyl-glucosaminoglycan obtained by alkaline deacetylation of chitin, is an excellent coating material known for its outstanding film forming properties with good mechanical performance and barrier capacity (Kurek,

Guinault, Voilley, Galić, & Debeaufort, 2014; Martins, Cerqueira, & Vicente, 2012). Besides that, several studies showed that chitosan had inherent antibacterial and antifungal properties, depends on its degree of deacetylation and molecular weight (Aider, 2010; Tan et al., 2015). In spite of the mechanical and antimicrobial properties, nevertheless, the single chitosan film did not present ideal antioxidant capacity (Liu et al., 2017). To meet out this challenge, various approaches have been tested for improving the coating film quality for better packaging of fresh produce by incorporating the natural antioxidant compounds, such as green tea extract and black soybean seed coat extract (Wang et al., 2018; Rubilar et al., 2013; Siripatrawan & Harte, 2010). In addition, natural antimicrobial agents have been used to develop the antimicrobial packages, including plant extracts such as grapefruit seed extract (Wang, Lim, Tong, & Thian, 2019), and whey protein (Brink, Šipailienė, & Leskauskaitė, 2019). As a natural biopolymer, chitosan was incorporated directly into meat products to inhibit microbial growth and to increase shelf-life of the meat products (Soultos, Tzikas, Abrahim, Georgantelis, & Ambrosiadis, 2008). Besides, it is common to blended chitosan with other polymers to obtain better packaging coating (van den Broek, Knoop, Kappen, & Boeriu, 2015). Recently, chitosan nanoparticles were used in delivery system of food packaging extending shelf-life of food (Lin, Xue, Duraiarasan, & Haiying, 2018). In this line, recently our group has introduced the idea of developing layer-by-layer (LBL) assembly of chitosan and carboxymethyl cellulose (CMC), which provide higher antioxidant and antimicrobial activities to the packaging film for postharvest fresh produce (Yan et al., 2019).

Following and expanding research with similar idea and considering MLT as a natural active antioxidant compound, the aim of the present work was to develop chitosan-based melatonin layer-by-layer assembly (CMLLA) as an innovative and active melatonin film formulation applicable to the post-harvested fresh products. Up to now, MLT-loaded polysaccharides assembly films have not been formulated and tested for its active role in fresh products. In the present study, the CMLLA was developed via the self-assembled molecular technique. The structure, color, biological and mechanical properties of the novel chitosan-based melatonin assembly were assessed. Further, to find the practical applicability of the developed films, the effect of CMLLA on quality attributes of three fresh-cut products were evaluated.

2. Material and methods

2.1 Materials

Food-grade chitosan (CH, deacetylation degree 91.0%) and carboxymethyl chitosan (CMCH, deacetylation degree: 91.0%) were bought from Golden-shell Pharmaceutical Co., Ltd, Zhejiang Province, and the carboxymethyl cellulose (CMC, viscosity: 800-1200mpa·s) was procured from Shanghai Aladdin Bio-Chem Technology Co., LTD

(Shanghai, China). Melatonin (MLT) (contains 10%-20% benzene, ≥97.0% HPLC), Acetic acid (98% HPLC), pure ethanol (95% HPLC) was purchased from Shanghai Aladdin Bio-Chem Technology Co., LTD (Shanghai, China). The 2,2-diphenyl-1-picrylhydrazyl (DPPH) was purchased from Sigma Chemical Co. (St. Louis, MO, USA). Deionized water (Millipore) was used to prepare the solutions. All other reagents were of analytical grade.

2.2 Preparation of CMLLA

The CH solution was prepared by dissolving chitosan powder in a 1% (v/v) aqueous acetic acid solution to obtain a chitosan concentration of 2.5% (w/v) in an assembly system. The CMCH and CMC solutions were prepared separately by dissolving 2.5g of each in 100 mL of deionized water to obtain the concentration of 2.5% (w/v) in an assembly system. All the solutions were homogenized by magnetic stirring for 2 h at room temperature until complete dissolution. To prepare the MLT-loaded assembly of CH, CH-M25, CH-M50, and CH-M100, which means MLT was added to CH solution at different concentrations of 0, 25, 50, 100 mg/L, respectively, and homogenized by magnetically stirring for 10 min.

The simple CH, CMCH and CMC, as well as the CH/MLT, CMCH/MLT assemblies were obtained by pouring the stock solutions into a glass dish. The solvents were removed by drying in a ventilated climatic chamber at 27 °C and 50% RH for 24 h. The dried surface was then peeled off and stored at 25°C and 53% RH until further analysis to obtain corresponding CMLLA. The CMLLA was prepared based on difference ratios of CH/CMCH to CMC stock solutions (1:4, 2:3, 3:2, and 4:1).

2.3 Structural characterization

The Fourier Transform-Infrared spectroscopy (FTIR) spectra of CMLLA were obtained by AVATAR370 FT-IR (Thermo Nicolet, USA). The crystalline characteristics were determined by X-pert powder diffractometer (Panalytical B.V., Netherland), which was operated at 40 mA and 40 kV using Ni-filtered Cu Kα radiation. The diffraction pattern was obtained from 2θ, 5° to 80° at a scan rate of 0.1° per second. A scanning electron microscope (SEM, HITACHI, Tokyo, Japan) was used to observe the cross-sectional microstructures of the films. The accelerating voltage of the SEM was 200 kV. The films were frozen with liquid nitrogen and pinched out with tweezers. The samples prepared were then fixed on individual specimen stubs and sputter-coated with gold. The cross-sectional photographs of the films were obtained at magnifications of 1000× and 10,000×, respectively.

2.4 Physical characterization

2.4.1 Thickness

The assembly thickness was measured by CHY-C2 Thickness Tester (PARM™, China).

The average values of five thickness measurements at different positions were used in all calculations.

2.4.2 Color and opacity

The color was determined by the CR-400 Chroma Meter (Konica Minolta Sensing, Inc., Japan). The L*(lightness), a* (red to green) and b* (yellow to blue) values were averaged from three readings for each sample. And then the total color difference (*ΔE*) was calculated as per the equation (1) (Gennadios, Weller, Hanna, & Froning, 1996):

$$\Delta E = \sqrt{\Delta L^{*2} + \Delta a^{*2} + \Delta b^{*2}} \quad \text{Eq. (1)}$$

where, ΔL*, Δ a* and Δ b* are the differences between the color parameter of the samples and those of the white standard (L*= 92.82, a* = −1.24, b* = 0.46).

The opacity was determined by measuring the film absorbance at 600 nm, using UV-5800PC spectrophotometer (METASH, China), following the method of Park et al. (2004). The film opacity was calculated by the absorbance against the thickness. All measurements were performed in triplicate.

2.4.3 Moisture content

CMLLA was cut into square pieces (20 mm × 15 mm) and the accurate weight (M_1) and the constant weight (M_2) was calculated. The moisture content was determined by the following equation (2):

$$\text{Moisture content (\%)} = (M_1 - M_2)/M_2 \times 100\% \quad \text{Eq. (2)}$$

2.4.4 Mechanical properties

The tensile strength (TS, in MPa) and percentage of elongation at the breakpoint (E, %) were determined by XLW (M) auto Tensile Tester (PARAM™, China), according to American Society for Testing Material (ASTM) standard method D882 (ASTM, 1992). Briefly, the assembly samples were cut into rectangular pieces (1 cm × 5 cm) and mounted in the extension grips of the testing machine and stretched axially at a rate of 50 $mm \cdot min^{-1}$. Three film specimens were used for each replicate.

2.5 Biological activities

2.5.1 Antioxidant capacity

The antioxidant capacity of the assembly was measured by DPPH radical scavenging assay (Mayachiew, Devahastin, 2010). Briefly, the assembly sample was stirred and dissolved in 10 ml of deionized water and mixed with DPPH reagent (150 *μ*mol/L). The absorbance was recorded at 517 nm for every 10 min in 2 h of reaction time. All measurements were performed for three replications.

2.5.2 Antimicrobial property

The antimicrobial properties of CMLLA were examined by the zone of inhibition assay on solid media as per the Seydim (2006) protocol with slight modifications. Three bacterials, *Salmonella Enteritidis* (*S. enteritidis,* ATCC 13076), *Escherichia coli (E. coli,* O157:H7, ATCC 35218), and *Listeria monocytogenes* (*L. monocytogenes,* NCTC 2167), which commonly present in fresh-cut products based on previous study, were used in antimicrobial assay (Fernandez-Saiz, Lagaron, & Ocio, 2009; Portes, Gardrat, Castellan, & Coma, 2009; Sánchez-González, González-Martínez, Chiralt, & Cháfer, 2010). Briefly, every 100 µL of bacterial cultures (colony count of 1×10^8 $CFUmL^{-1}$) inoculated in 10 mL of molten LB nutrition agar. Test discs were placed on the bacterial lawns. The plates were incubated at 37°C for 24 h. The diameter of the test discs was 10mm. The diameter of the zone of inhibition was measured with a caliper. The average value of the zone of inhibition was calculated as the means of three measurements.

2.6 CMLLA on quality traits of fresh produce

Fresh produce of *Cucumis sativus* (cucumber)*, Brassica oleracea* (broccoli) and *Cucumis melo* (melon) in uniform color and size without mechanical injury were selected and cut into ready-to-eat pieces and subjected to different treatments (control (pure water), According to the previous study of Yan et al. (2019), the control group was immersed in distilled water for 30 s, the single layer group was immersed in the 1.2% CH/CMCH solution for 30 s, and the CMLLA group was first coated with CH/CMCH solution under different concentration and dried at room temperature for 20-30 min, and then coated with CMC (Table 1). After the produce surface was completely dry, all samples placed in the plastic casing at room temperature Based on the properties of fresh products and Accelerated Shelf-life Test (ASLT), storage time was 5 days for cucumber, 7 days for broccoli and 5 days for melon, respectively, All quality attributes below were determined for three technical replications and three biological replications. The weight loss of the ready-to-eat produce was calculated by comparing the initial and final weight (Sathivel, 2005). The firmness was measured using a TA-XT2i texture analyzer (Stable Microsystems Texture Technologies Inc., UK) with a cylindrical probe (5 mm diameter) with the test speed of 0.5 mm s^{-1} and a pierce distance of 5 mm. Firmness was tested at three locations on each fruit and the result was expressed as the maximum compression force (g). The content of titratable acidity (TA) and total soluble solids (TSS) was measured using a PLA-1 pocket refractometer (ATAGO CO., Tokyo, Japan). The juice from fruit samples was squeezed out and used immediately for determining TA and TSS concentration. The color of the ready-to-eat produce was determined by CR-400 Chroma Meter (Konica Minolta Sensing, Inc., Japan). Furthermore, the chlorophyll content in broccoli was measured by recording the absorbance at 663 nm and 645 nm using a UV-5800PC spectrophotometer (METASH, China).

Table 1. Assembly with different components in the present study.

Assembly	Addition of components		
	CH/CMCH (%)	CMC (%)	MLT (mg/L)
Control	0	0	0
CH/CMCH	1.2	0	0
CH-M25	2.4	1.6	25
CH-M50	2.4	1.6	50
CH-M100	2.4	1.6	100
CH/CMCH1.2	1.2	0.8	50
CH/CMCH1.8	1.8	1.2	50
CH/CMCH2.4	2.4	1.6	50

2.7 Statistical analysis

The results were analyzed by the statistical software SPSS ver. 18.0 (SPSS Inc., Chicago, IL, USA). All data was expressed as means ± standard deviations (SD) from three technical and biological replications. One-way analysis of variance (ANOVA) with a 95% confidence interval of the data was conducted using SPSS 18.0 (SPSS Inc., Chicago, IL, USA).

3 Results and discussion

3.1 Structural Characterization

3.1.1. FTIR analysis

FTIR spectroscopy was carried out to demonstrate the interactions between CH/CMCH and CMC. In this study, three represented samples are shown to demonstrate the structure of CMLLA. Fig. 1 showed the FTIR spectra for the CH, CMCH, CMC, CH-CMC (3:2) and CMCH-CMC (3:2) assemblies.

The main bands observed in the CH spectrum (Fig. 1) were: (i) a broad asymmetric band between 3400 and 2500 cm^{-1} corresponding to the axial stretching of C-H bonds; (ii) a region between 1700-1200 cm^{-1} attributed to the amide groups; (iii) a strong absorption region between 1200-800 cm^{-1} due to the polysaccharide skeleton, including the vibration of the glycoside bonds, C-O and C-O-C stretching (Zhai et al., 2017; Branca et al., 2016; de Abreu & Campana-Filho, 2009; Wang et al., 2005). It was demonstrated in Fig. 1 that the structural difference between the CH spectrum and the carboxymethylated CMCH, (i) the broader band centered at 3300 cm^{-1} which revealed the more hydrophilic characterization of CMCH; (ii) the presence of an intense band in 1630 cm^{-1} and a moderate band at 1423 cm^{-1}, were contributed to the symmetric and asymmetric axial

deformation of COO, respectively (Bao et al., 2014; de Abreu & Campana-Filho, 2009; Esteghlal, Niakousari, & Hosseini, 2018). In the CMC spectrum, the characteristic bands in 3423 cm^{-1} and 2921 cm^{-1} were assigned to -OH and -CH stretching regions, respectively (Fig. 1). The characteristic absorption bands of symmetric and asymmetric -COO were observed in 1418 cm^{-1} and 1605 cm^{-1}, respectively. These characteristic absorption bands are consistent with that in previous studies (Esteghlal, Niakousari, & Hosseini, 2018).

In the spectrum of CH-CMC sample (Fig. 1), the region between 3400 and 2000 cm^{-1} with a clear increase in the intensity of the bands, indicating the amino proton was synthesized to be NH_3^+ in the film. The band of N-H stretching vibration was shifted to 3420 cm^{-1}, indicate hydrogen bond association. The C=O and N-H groups were overlapped with a shift of C-O stretching vibration to 1410 cm^{-1}, showed the existence of COO^-, indicating the intermolecular hydrogen bonding of C=O…H-N between two materials. The peak of C-H at 2926 cm^{-1} became weaker, attributing to the intermolecular interaction between CH and CMC (Boy et al., 2016). In the CMCH-CMC spectrum, the overlapped bands at 1581 cm^{-1} are associated with the asymmetric stretching of carboxylic anion COO^- and the stretching of the amino group. The absorption at 1065 cm^{-1} attributed to C-O-C pyranose ring vibration in CMCH and CMC (Esteghlal, Niakousari, & Hosseini, 2018; Yang, Yan, Chen, Lee, & Zheng, 2007). Besides, the peak of amide III in the spectrum of CMC-CMCH film at 1322 cm^{-1} of C-H became weaker, indicating a replacement of the amino group and these results indicated the presence of heterocyclic amine and ester bond in CMLLA.

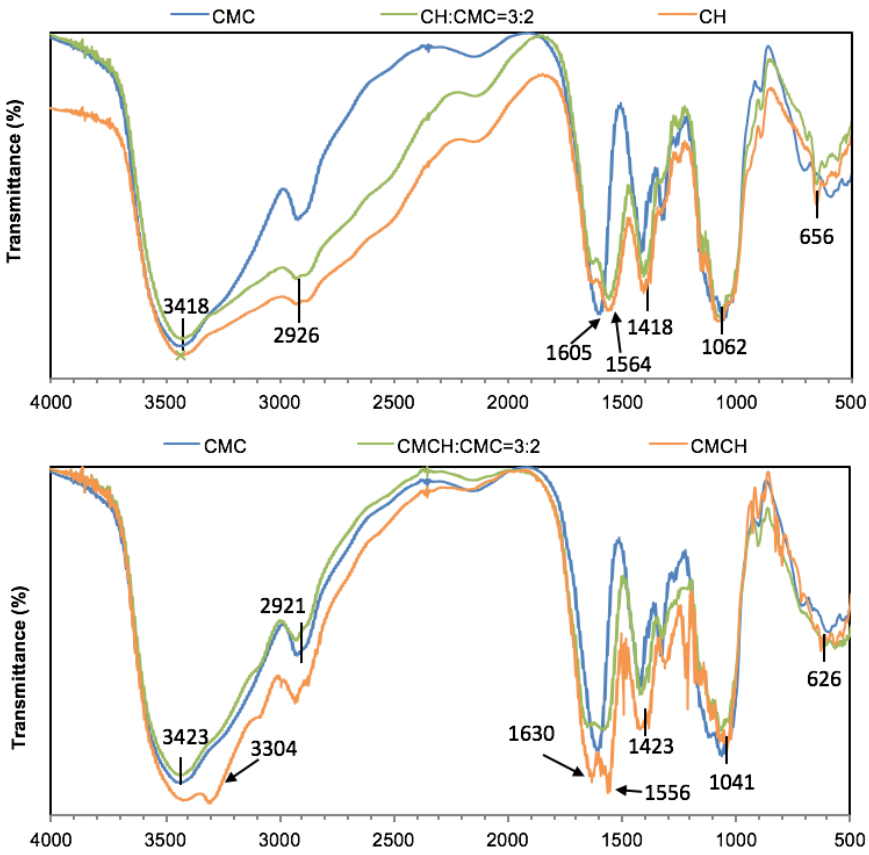

Fig. 1. FT-IR spectra of CMLLA films. (a) CH/MLT-CMC; (b) CMCH/MLT-CMC

3.1.2. XRD patterns

Crystalline characteristics of CMLLA were determined by XRD. As shown in Fig. 2, the simple chitosan film presented a semi-crystalline characteristic with diffraction peaks at 11.7°, 14.2° and 17.0°, which were similar to the previous studies (Liu et al., 2017; Tan et al., 2015). The diffraction peak at 11.4° was owing to the hydrated crystalline structure, while the broad peak at 20°-23° represented the amorphous structure of chitosan (Rivero et al., 2010). Compared with CH, the spectrum of CMCH exhibited poorly defined and less intense peaks, which was resulted from the presence of carboxymethyl groups substituting the hydrogen atoms of the hydroxyl and amino groups (de Abreu & Campana-Filho, 2009).

When incorporated with CMC into the CMLLA, the broad peak became wider and weaker. It was demonstrated that the overall crystallization rate was low, as the intensity of the crystal peak of CH at 20° (2θ) declined significantly, compared to CH. Furthermore, it was proved that the molecular chains of both crystalline polymers without presence of crystallization, of which the domains of both components were scarcely formed (Sakurai et al., 2000). Therefore, the amorphous nature of the CMLLA further confirmed the good miscibility of the components. This was probably due to the intermolecular interaction between hydroxyl groups and NH_3^+ in CMC and chitosan, which limited the molecular

movement of both chitosan and CMC (Mathew & Abraham, 2008; Liu et al., 2016). These results further strongly predicted the good compatibility of two constituents in CMLLA. Presence of CMC induced the looseness of chitosan structure, resulting in a matrix more unlikely to hydrogen bonding formation and leading to the decrease of the crystallinity.

Block backbone model was built to illustrate the tentative interaction mechanisms between CH and CMC (Fig. 3). The model showed that the two components would have hydrogen bonding and amidation to form a complex network. The OH group of CMC molecules interacted with OH groups of chitosan, leading to a matrix less favorable to hydrogen bonding with water which in turn would decrease moisture content of CMLLA. In the model, there are C=O…H-N intermolecular hydrogen bonding between two materials. Therefore, compared to the molecular distance of simple chitosan film, CMLLA showed obvious differences and the latter might be slightly looser than the former (Feng, Liu, Zhao, & Hu, 2012; Okuyama et al., 2000). The much loose arrangement of CMLLA might facilitate the penetration of water molecules.

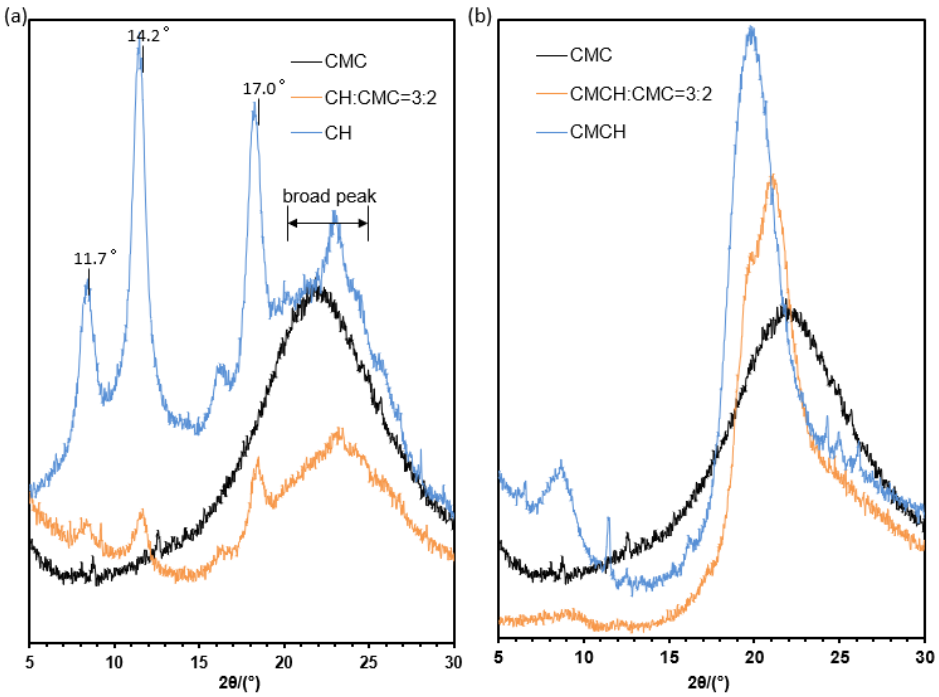

Fig. 2. XRD patterns of CMLLA films. (a) CH/MLT-CMC; (b) CMCH/MLT-CMC

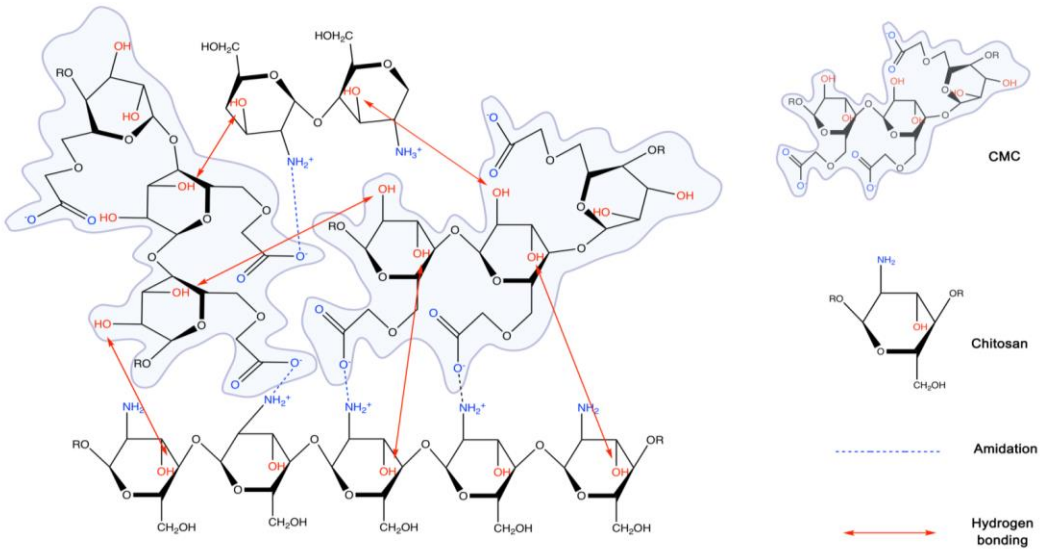

Fig. 3. The built block backbone model to illustrate the tentative interactions between CH and CMC.

3.1.3. Microstructural analysis

The microstructure of cross-section of CMLLA was investigated by SEM. Fig. 4 showed the microstructure of cross-section of the film (CH:CMC = 1:4, 2:3, 3:2) which can provide information about different components and interaction between two constituents. The surface of the plain chitosan film showed a smooth and uniform appearance (Fig. 4a). The intersection of CH-CMC film appeared somewhat rough (Fig. 4d), which may be due to the interaction between chitosan and CMC. In previous studies, similar results were reported which showed chitosan-Sodium alginate (SA) films had rough surface between intersection which indicated less homogeneity of the components owing to the positive and negative charged interactions (Li et al., 2019; Sogut, & Seydim, 2018). The film's morphologies had an obvious difference compared to the different ratio of film's constituents (Fig. 4). Among all the films tested, film (CH:CMC=1:4, 2:3) had obvious fracture surface in the intersection (Fig. 4d, e), while film (CH:CMC=3:2) was more uniform and smooth (Fig. 4f), probably due to the interaction between chitosan and CMC. In the study of Sogut et al. (2018), the addition of nano-cellulose (NC) into CH up to 10% resulted in a smooth surface in the cross-section of the bilayer films, which can effectively enhance the properties of CH due to the similarity of cellulose CH (Khan, Huq, Khan, Riedl, & Lacroix, 2014).

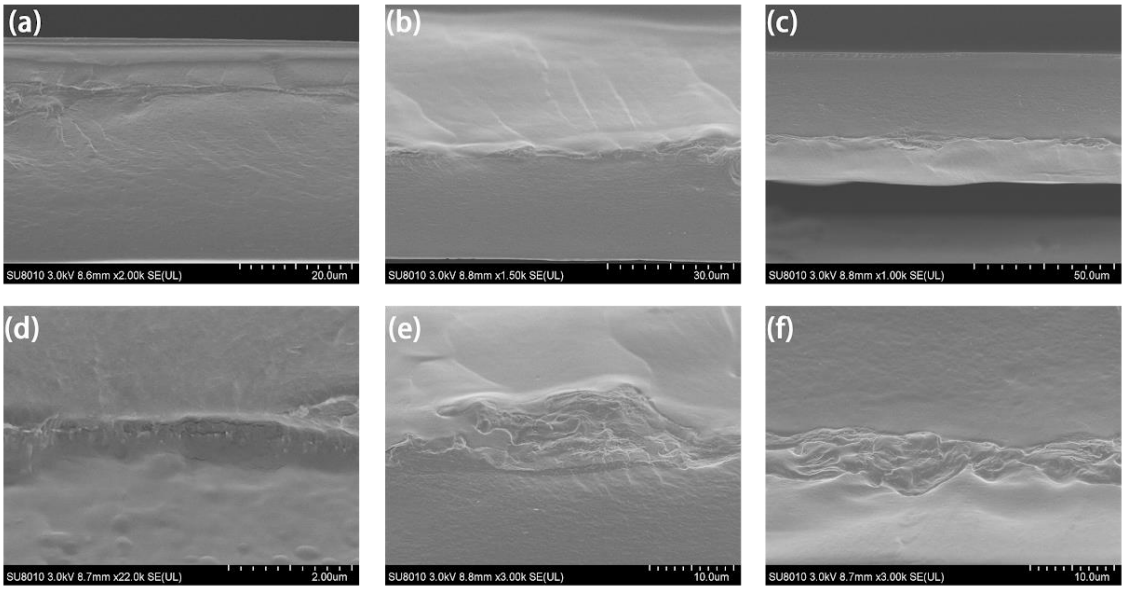

Fig. 4. Scanning electron microscope images of CH:CMC=1:4 at 1,500× (a) and 220,000× (d) magnification, CH:CMC=2:3 at 1,000× (b) and 10,000× (e) magnification, and CH:CMC=3:2 at 1,000× (c) and 10,000× (f) magnification.

3.2 Physical characterization

3.2.1 Opacity and color

Color is an important property of assembly appearance. Assembly with different ratio of chitosan and CMC were prepared to verify color changes of samples. Fig. 5 showed the morphology and visible color variation of CMLLA. Color and opacity parameters of films were summarized in Table 1. Results showed that bilayers under different ratio had a significant distinction in color and opacity (p<0.05). The film color was visibly changed from pale white with low opacity for CMC film to yellow for CH, and high opacity for CMCH, respectively (Fig. 5). The color of pure chitosan was associated with the carotenoid pigment astaxanthin (Kucukgulmez et al., 2011) and the preparation procedure (Seo, King, & Prinyawiwatkul, 2007). The color difference increased with the increasing ratio of chitosan, with ΔE ranging from 8.24 for the assembly (CH:CMC = 1:4) to 12.10 for the assembly (CH:CMC = 5:0). However, the increased ratio of chitosan had little influence on the opacity of assembly. In CMCH-CMC assembly, the opacity significantly increased when the ratio of CMCH increased (p<0.05).

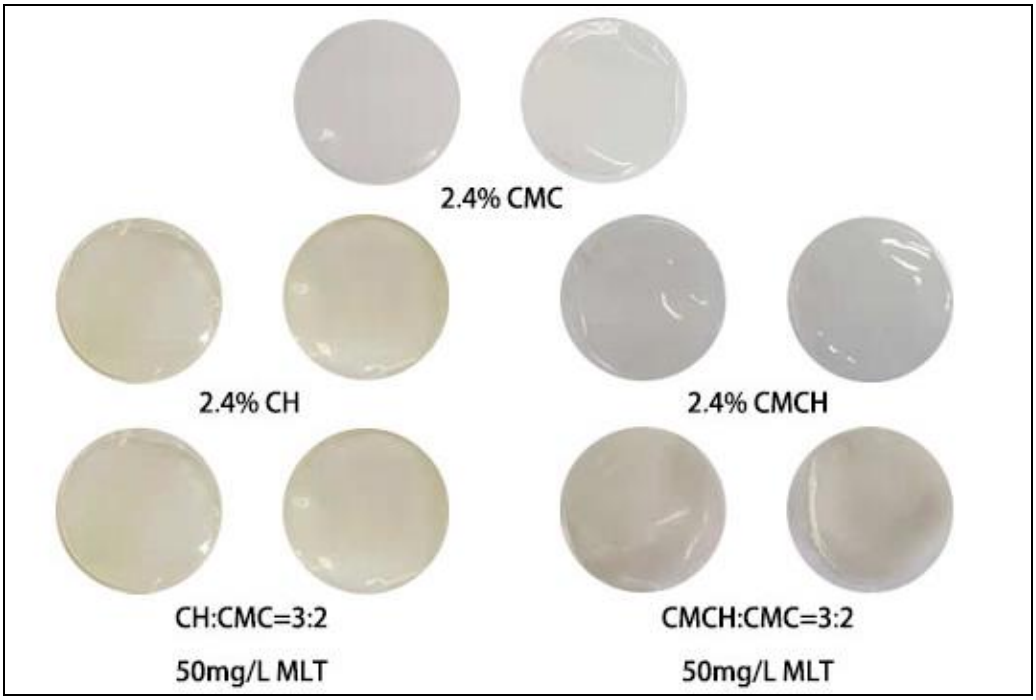

Fig. 5. Morphology of CMLLA samples.

3.2.2 Mechanical properties

The mechanical properties of CMLLA included tensile strength (*TS*), elongation at break (*E*), thickness (*T*), and moisture content (*MC*) were shown in Table 1.

CH had the lowest *TS* (54.42±3.67 MPa) and this value increased with the increasing CMC concentration, which increased twice than the simple CH. Similarly, reports indicated that when CH was combined with CMC, the *TS* increased by 150% (Marzieh, 2019). In the previous research from Zhuang et al. (2018), nevertheless, the mechanical strength of LBL assembly was 38.27% lower than that of single-layer sodium alginate (SA), which probably due to the materials of the bilayers that had bad compatibility with each other. On the contrary, simple CH has higher *E* value, while the combination with CMC would decrease the *E* value, which might be caused by the entanglement and interaction between two polymer constituents. It has been proved that the mechanical behaviors had a close relationship with the inner structure (Wu et al., 2016). Results of the present study showed that CH-CMC assembly exhibited higher *TS* and lower *E* values which might be owing to the hydrogen bonding and electrostatic interaction between the positively charged CH and negatively charged CMC (Fig. 3).

The thickness of CMLLA is given in Table 1. As expected, CMLLA exhibited higher thicknesses than simple chitosan and CMC films; and the average thickness of films increased gradually with the increase in the ratio of chitosan. The average thickness of CMLLA (CH:CMC = 4:1) was 75.3 μm, which was 1.91 times thicker than simple CMC film. This might be due to the intersection of CH and CMC, which can be also seen in SEM

images (Fig. 4).

The moisture content (*MC*) of CMLLA was shown in Table 1. It was widely suggested that the higher *MC* of simple chitosan film was due to the strong hydrogen bond interactions with water molecules (Aljawish et al., 2016). *MC* of assemblies reduced from 15.72% to 12.68%, when the ratio of chitosan increased from 0% to 40%. Compared with simple chitosan and CMC, CH-CMC assemblies exhibited lower moisture contents which might be owing to the hydroxyl and carboxyl groups in CMC molecules which interact with the hydrophilic groups in chitosan (Marzieh et al., 2019). It was revealed that the CMLLA (CH:CMC = 3:2) exhibited the best physical properties compared with other samples. CH-CMC assembly maintained better mechanical properties with average thickness of 69.8 μm for CH and 56.1 μm for CMCH, and the opacity significantly as the CH ratio increased (p<0.05).

388 **Table 2.** Mechanical properties (*T*, Thickness, *E*, Elongation at break, *TS*, Tensile strength, *MC*, Moisture content), opacity and color changes (ΔE) of

389 CMLLA films (average ± standard deviation).

	CH						CMCH					
	T (μm)	*E* (%)	*TS* (MPa)	*MC* (% H_2O)	Δ*E*	Opacity	*T* (μm)	*E* (%)	*TS* (MPa)	*MC* (% H_2O)	Δ*E*	Opacity
0:5[#]	39.4±3.4^{a*}	1.90±0.013^{a}	64.91±20.31^{b}	13.97±0.03^{ab}	6.98±0.12^{a}	1.452±0.030^{a}	39.4±3.4^{a}	1.90±0.013^{a}	64.91±20.31^{b}	13.97±0.03^{a}	6.98±0.12^{a}	1.452±0.030^{a}
1:4	54.4±3.1^{b}	1.90±0.013^{a}	52.27±6.67^{a}	16.31±0.01^{b}	8.24±0.31^{a}	1.225±0.337^{a}	39.1±7.3^{a}	5.71±0.040^{ab}	42.75±5.94^{ab}	15.63±0.01^{a}	8.00±0.06^{b}	1.422±0.176^{a}
2:3	66.7±10.8^{bc}	3.81±0.013^{ab}	58.91±5.63^{a}	12.68±0.01^{a}	9.78±0.66^{b}	1.407±0.162^{a}	48.1±4.3^{ab}	1.90±0.013^{a}	55.81±15.95^{ab}	12.65±0.02^{a}	8.36±0.46^{bc}	1.909±0.642^{a}
3:2	69.8±8.4^{c}	8.57±0.040^{b}	48.38±1.48^{a}	15.58±0.01^{b}	10.13±0.45^{b}	2.143±0.282^{ab}	56.1±3.4^{b}	7.62±0.013^{b}	43.41±5.20^{ab}	15.10±0.01^{a}	8.79±0.30^{c}	6.802±1.114^{b}
4:1	75.3±8.4^{c}	2.86±0.00^{a}	60.36±9.23^{ab}	14.11±0.01^{ab}	11.58±1.26^{c}	2.279±0.259^{b}	62.5±13.6^{b}	6.67±0.013^{ab}	44.55±0.56^{ab}	14.51±0.01^{a}	10.21±0.19^{d}	8.243±0.980^{c}
5:0	57.7±9.6^{b}	3.81±0.013^{ab}	54.42±3.67^{a}	15.72±0.00^{b}	12.10±1.48^{c}	1.274±0.145^{a}	46.7±7.0^{a}	10.48±0.049^{b}	34.49±10.25^{a}	16.46±0.04^{ab}	10.67±0.66^{d}	12.384±1.620^{d}

[#]Different proportion means the ratio of CH/CMCH and CMC.

*Different superscripts (a-d) within a column indicate significant differences among samples ($p<0.05$)

3.3 Biological activities

3.3.1 Antioxidant capacity

The free radical scavenging ability of the packaging films is usually required for active packaging of fresh produce. The DPPH antioxidant activity of CMLLA was shown in Fig. 6. The addition of MLT significantly increased the antioxidant capacity of CH-CMC assembly. Compared with single chitosan film, the DPPH radical scavenging activity increased with increasing of loaded MLT concentration and release time in assemblies. Nevertheless, the DPPH radical scavenging activity of CH-MLT50 and CMCH-MLT50 were 45.55% and 30.67%, respectively. The result showed the higher antioxidant activity in CH film which was different from previous studies (Guo et al., 2005; Zhao, Huang, Hu, Mao, & Mei, 2011; Chen et al., 2015). The difference of antioxidant capacity was resulted from the different solvent used for preparation of MLT stock solution. The introduction of carboxymethyl groups into the chitosan, could increase the hydrogen-donating ability which actively scavenged the DPPH radicals (Chen, & Ho, 1995; Zhao, Huang, Hu, Mao, & Mei, 2011) (Lee, 2016). Compared with chitosan, CMCH had the significantly improved antioxidant capacity, which probably due to the modified structure of CMCH. Moreover, the control samples were shown the lower DPPH scavenging activity, which was consistent with that in previous studies (Sun et al., 2017; Yen, Yang, & Mau, 2008). The exogenous addition of MLT significantly increased the antioxidant capacity of CH/CMCH-CMC assembly. And the antioxidant capacity of CH-MLT50 and CMCH-MLT100 increased by 2 folds compared to the control. Moreover, the DPPH radical scavenging activity of CH-MLT50 and CMCH-MLT50 were 45.55% and 30.67%, respectively.

Moreover, the study presented that antioxidant capacity increased slowly at first, nevertheless, there was a significant difference between assemblies with or without addition of MLT (p<0.05). It was probably due to the viscosity of CH/CMCH, which leads to the controlled release of MLT.

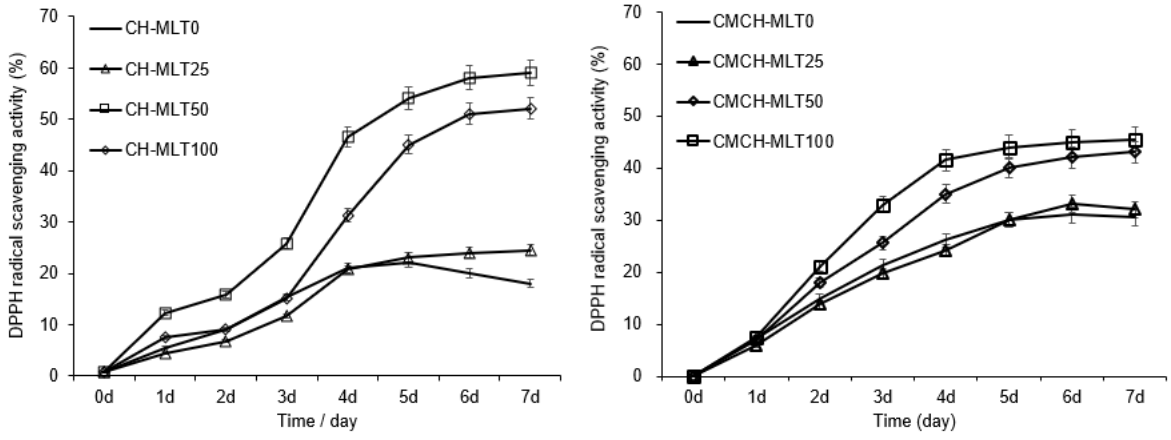

Fig. 6. Antioxidant capacity of CMLLA incorporated with different concentration of

melatonin.

CH, CH: CMC=3:2, CMCH, CMCH: CMC=3:2, MLT0, C_{MLT}=0 mg/L, MLT25, C_{MLT} =25 mg/L; MLT50, C_{MLT} =50 mg/L; MLT100, C_{MLT} =100 mg/L.

3.3.2 Antibacterial property

The zone of inhibition assay was employed to investigate the antibacterial property of CH/MLT and CMCH/MLT assemblies against *S. enteritidis, E. coli,* and *L. monocytogenes.* The inhibitory effect of CMLLA on the growth of three kinds of microorganisms was shown in Fig. 7. Results revealed that there was little difference in inhibition zones between control and MLT23. These results indicated the original antimicrobial property of CH and CMCH. Consistently, Fernández-Saiz et al. (2013) also observed that chitosan could inhibit the microbial growth in hake fillets when packaged in air and under vacuum. The bacterial activity of CH might be owing to the free amino groups and the electrostatic interaction. Binding to cell surface, disturbing the cell membrane, the amino groups may cause the cell death by inducing leakage of intracellular components (Chung & Chen, 2008; Wahid et al., 2016). According to the study of Sayari et al. (2016), generally, the chitosan exhibited higher antimicrobial activities on gram-positive bacteria than that on gram-negative bacteria, which leading to the discrepancy of inhibition zone. And the order of the antimicrobial activities of CMLLA against microorganisms was: *E. coli* < *L. monocytogenes* < *S. enteritidis,* which was consistent with that in previous study (Jeon, 2001; Sun et al., 2017).

Furthermore, the MLT loading in the CMLLA delivery system increased the antibacterial activity. It has been widely proved the antibacterial effect of MLT against gram-positive and gram-negative bacteria, which ascribed to its ability to reduce intracellular substrates availability such as free iron and fatty acids (Romić et al., 2016), although most research of MLT was limited in the clinical study relevant to wound healing (Tekbas, Ogur, Korkmaz, Kilic, & Reiter, 2008; Vielma et al., 2014). Our study showed that exogenous MLT may effectively inhibit the growth of three presentative microorganisms. The inhibition zone of CH-MLT100 against *S. enteritidis* was 1.83 cm, which was 1.31 times larger than that of control (Fig. 7). All above results provided evidence that the antimicrobial activities of CMLLA resulted from the synergic application of both CH and MLT. Result of the positively antimicrobial properties indicated that the CMLLA could potentially be applied as antimicrobial packaging materials in maintenance of quality attributes.

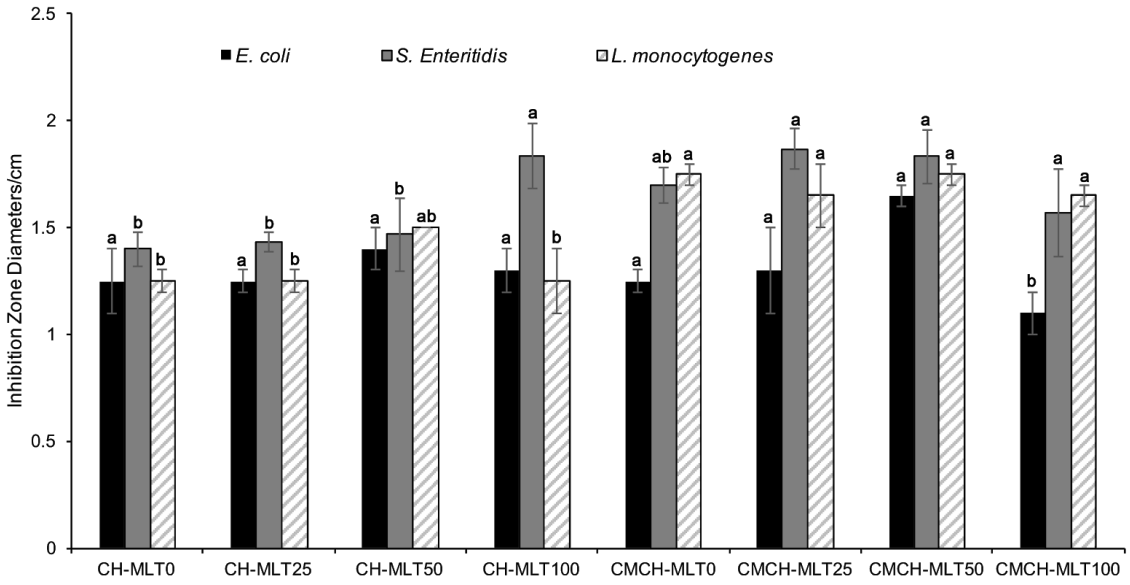

Fig. 7. Antibacterial activity of CMLLA samples.

CH, CH: CMC=3:2, CMCH, CMCH: CMC=3:2, MLT0, C_{MLT}=0 mg/L, MLT25, C_{MLT} =25 mg/L; MLT50, C_{MLT} =50 mg/L; MLT100, C_{MLT} =100 mg/L.

3.4 CMLLA on quality traits of fresh produce

3.4.1 Cucumber (*Cucumis sativus*)

Morphological characteristics of cucumber was exhibited in Fig. 8. As expected, the surface of cucumber coated by CH was much whiter and rougher than control. And CMCH coating contributed to the smooth and opaque morphology. Moreover, CMLLA better maintained the appearance (Fig. 8a). The quality attributes of cucumber in response to MLT-incorporated assembly were shown in Table a. Firmness was improved by 1.67 times by CH1.2 than control, while in CMCH2.4 the firmness was 21.40% lower than control. During postharvest storage, the sugar-acid ratio of cucumber decreased gradually. In comparison to control, LBL coating significantly prevent the decrease in sugar-acid ratio, which was 1.58 in CH1.2 group, and about 41.07% higher than control. And ΔE (Table 2) showed that CH1.2 had minimal variation which was 57.2% lower than control.

Results revealed that CMCH (14.35%) had much more weight loss than CH (10.80%), which might be due to the water solubility of CMCH that increase the loss of water on the surface of cucumber produce. And compared with CH, CMCH increased the sugar content by 9.1%. Furthermore, the viscosity of high concentration of CH and CMCH applied in assembly contributed to the decrease of the oxygen and water vapor permeability, and then accelerated the decomposition rate of the post-harvested cucumber. The incorporation of loaded MLT would largely retain the sugar, firmness and color in cucumber, which was consistent with the research reported by Xin et al. (2017), where the cucumber was treated by MLT-incorporated assembly. Results revealed that

MLT could effectively better maintain the sensory properties of postharvest *Cucumis sativus* and retard the decrease of TA, which indicated the better-quality maintenance of the MLT loaded films.

3.4.2 Broccoli *(Brassica oleracea)*

Morphological characteristics of broccoli were presented in Fig. 8b. Compared with the control group, the color of broccoli florets was much brighter and much greener when coated with MLT film. However, the effect of MLT was suppressed when incorporated with CH under high concentration, which accelerated the decline in the quality of broccoli, along with increased bacterium infection and yellowing problem. The quality attributes of broccoli were shown in Table 2. During postharvest storage, LBL coating dramatically retards the decrease of firmness and weight. The firmness of low concentration (1.2%, 1.8%) of CH is 1.51 and 1.33 times harder than control. The weight loss of CH1.2 was only 12.89%, which represent 42.89% lower than that of control. Furthermore, the results of high concentration coating of broccoli were similar as for cucumber. There is no difference in weight loss between control and CH2.4, however the color change of CH2.4 (ΔE=9.95) increased significantly (p<0.05).

Loss of green color of broccoli florets is one of the important factors which influence the quality of post-harvested produce. Takeda et al. (1993) reported more than 80% reduction in chlorophyll in broccoli florets within 4 days when stored at 23 °C. The present study results revealed that coating can effectively attenuate the decrease of chlorophyll concentration. Compared to control, treatment of MLT can mediate the decline of chlorophyll a (Table 2). The level of chlorophyll a in control treatment declined from 4.33 μg mg^{-1} on day 0 to 2.93 μg mg^{-1} on day 3. And the level of chlorophyll a in CH1.2 and CH1.8 is 1.95 and 1.89 times higher than control, respectively, manifesting the significant effect of MLT to maintain the color of *Brassica oleracea* (p<0.05). These results are in agreement with other studies on coating fresh-cut vegetable samples (María V. Alvarez et al., 2013; Zhang J et al., 2017; Arnao, M.B., Hernández-Ruiz, J, 2009). For instance, Arnao, M.B., Hernández-Ruiz, J (2009) reported that the chlorophyll loss in barley leaves slowed down when treated with MLT. The present results revealed that the quality of postharvest *Brassica oleracea* would be largely retained by the application of MLT. This might be due to the higher antioxidant activity of the MLT film which prevents the chlorophyll degradation.

3.4.3 Melon *(Cucumis melo var. saccharinus)*

Morphological characteristics of melon were shown in Fig. 8c. In control group, melon showed loss of water and softness of tissue, which prevent them to keep in its original form. However, melon coated with CMLLA had a better appearance and sensory

properties. Table 2 showed that the melon quality corresponding to CMLLA. Tissue softening occurs in melons during storage, and associated to the changes in the structure, composition and linkages, which further contributed to its decreased weight and firmness (Li et al., 2013a; Ortiz et al., 2011). Weight loss was declined in case of CMCH1.2 and CMCH1.8, which was 46.19% and 36.11% lower than control, respectively. And firmness in CH1.2 was improved by 9.28 times than control. Fresh-cut melons, as we knew, are prone to quick physiological and microbial deterioration resulted in softening and juice loss (Elena et al., 2018). Similar studies had been reported that coatings physically enhanced the structure of melon and slowed down their degradation (Baldwin, Hagenmaier, & Bai, 2011). And many researchers had pointed out that coating with chitosan could effectively prevented weight loss due to a stable and uniform barrier created by chitosan coatings (Kader, 2002; Ochoa-Velasco et al., 2014; Ali et al., 2011).

TSS under different treatments showed significant differences (p<0.05). Coating groups had significantly higher TSS values when compared with control groups. The level of TSS in the control group was declined from 16.32% to 11.43%. And low concentration (1.2%, 1.8%) CH showed TSS 1.23 and1.25 times higher than control, respectively. The similar results of MLT coating on fresh-cut fruits were reported elsewhere (Gao et al., 2016; Ma et al., 2016; Liu et al., 2018; Liu et al., 2016). For instance, Liu et al. (2016) reported tomato fruits treated with MLT have higher soluble solid and sugar contents than control. These results indicated that MLT can increase fruits ability to resist oxidative stress and then delay postharvest senescence (Ma et al., 2016). Results showed that under treatment of MLT-incorporated assembly, sensory properties of melon would be largely maintained and decrease of TSS would be retarded.

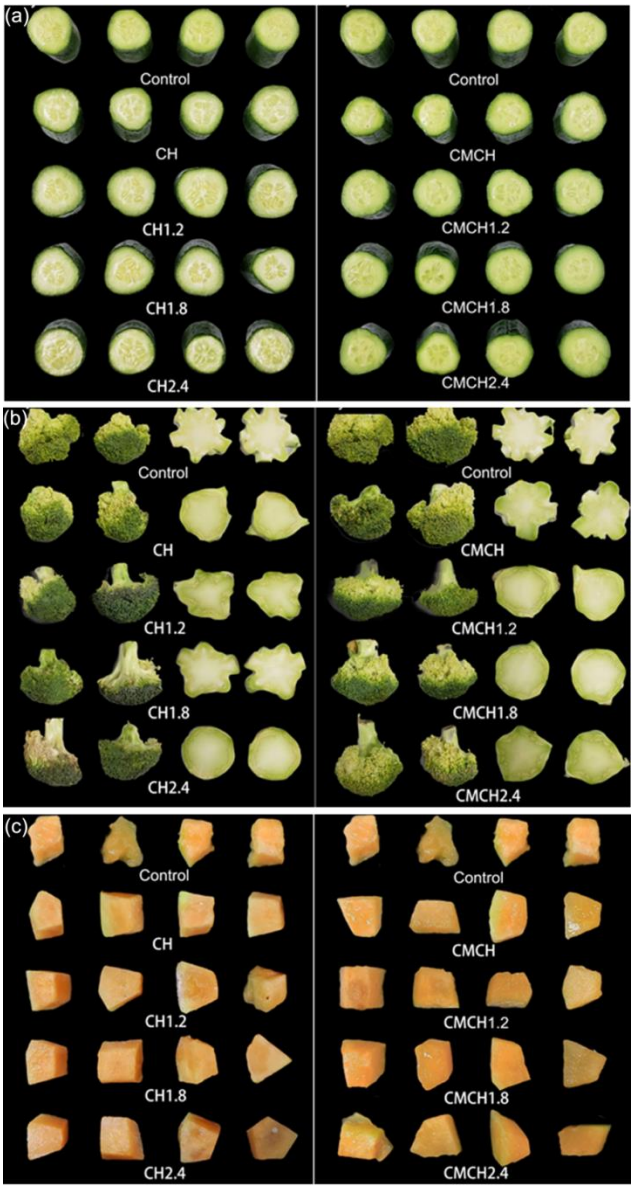

539

540 **Fig. 8**. Impact of CMLLA on morphological characteristics of fresh products

541 **Table 3.** CMLLA on quality attributes of *Cucumis sativus, Brassica oleracea,* and *Cucumis melo* (average ± standard deviation)

	CH						**CMCH**					
Cucumis sativus	Weight loss /%	Firmness /g		Sugar-acid ratio	ΔE		Weight loss /%	Firmness /g		Sugar-acid ratio	ΔE	
		Section of fruit	Section of center					Section of fruit	Section of center			
Control	18.81±3.33^{b*}	1322.83±35.73^{a}	344.87±34.50^{b}	1.15±0.12^{a}	7.72±0.81^{c}		18.81±3.33^{b}	1322.83±35.73^{a}	344.87±34.50^{a}	1.15±0.12^{a}	7.72±0.81^{b}	
CH/CMCH	16.32±0.76^{b}	2075.83±22.37^{c}	425.00±12.59^{c}	1.49±0.06^{bc}	6.48 ±0.60^{a}		19.02±2.04^{b}	1914.37±92.55^{a}	499.58±36.01^{a}	1.37±0.03^{b}	6.62±0.79^{ab}	
C1.2$^{\#}$	10.80±0.70^{a}	2157.20±33.46^{c}	631.63±90.08^{c}	1.58±0.09^{c}	4.72±0.35^{b}		12.35±0.83^{a}	1955.10±62.81^{b}	440.67±11.36^{a}	1.74±0.08^{c}	6.10±0.40^{a}	
C1.8	11.58±0.84^{a}	2210.33±149.26^{c}	467.33±24.91^{c}	1.41±0.04^{b}	5.11±0.63^{b}		11.33±0.42^{a}	1943.37±17.06^{a}	657.80±120.72^{b}	1.50±0.03^{b}	7.37±0.28^{b}	
C2.4	17.06±0.68^{b}	1576.43±101.11^{b}	405.23±61.81^{a}	1.47±0.16^{bc}	7.57±0.87^{c}		13.01±0.97^{a}	1038.93±14.09^{a}	293.27±148.34^{a}	1.16±0.17^{a}	7.45±0.59^{b}	
Brassica oleracea	Firmness /g	Weight loss /%		Chlorophyll concentration /mg/L		ΔE	Firmness /g	Weight loss /%		Chlorophyll concentration /mg/L		ΔE
		Flower	Stem	Chlorophyll a	Chlorophyll b			Flower	Stem	Chlorophyll a	Chlorophyll b	
Control	2548.80±121.57^{a}	32.54±4.26^{b}	18.64±0.29^{c}	2.93±0.13^{a}	2.54±0.23^{a}	6.86±0.19^{b}	2548.80±121.57^{a}	32.54±4.26^{c}	18.64±0.29^{b}	2.93±0.13^{a}	2.54±0.23^{a}	6.86±0.19^{b}
CH/CMCH	3578.90±88.57^{b}	23.40±4.01^{a}	19.31±0.98^{c}	3.21±0.06^{b}	2.45±0.10^{a}	6.50±1.34^{b}	3768.03±77.25^{c}	26.81±3.52^{b}	16.82±2.88^{b}	3.25±0.18^{b}	2.88±0.26^{a}	6.09±1.04^{b}
C1.2	3859.27±50.20^{c}	24.42±2.91^{a}	12.89±1.07^{ab}	5.72±0.09^{c}	3.78±0.26^{b}	4.03±0.56^{a}	4392.10±146.14^{d}	16.64±2.54^{a}	11.93±0.36^{a}	4.19±0.25^{d}	3.98±0.26^{b}	3.96±0.83^{a}
C1.8	3397.30±165.25^{b}	22.38±4.00^{a}	10.72±0.28^{a}	5.55±0.13^{c}	4.12±0.27^{b}	3.07±0.90^{a}	3722.80±182.94^{c}	16.69±2.19^{a}	10.07±1.32^{a}	3.72±0.03^{c}	3.69±0.06^{b}	2.93±0.61^{a}
C2.4	3427.73±152.29^{b}	40.79±6.72^{c}	14.62±1.94^{b}	2.99±0.15^{a}	2.43±0.26^{a}	4.39±0.21^{a}	3060.17±310.54^{b}	19.12±2.61^{a}	14.00±1.55^{ab}	3.79±0.08^{c}	2.72±0.18^{a}	9.55±1.12^{c}
Cucumis melo	Firmness /g	TSS /%		Weight loss %	ΔE		Firmness /g	TSS /%		Weight loss /%	ΔE	
Control	67.43±12.48^{a}	11.43±0.60^{a}		29.55±7.48^{b}	12.74±0.84^{d}		67.43±12.48^{a}	11.43±0.60^{a}		29.55±7.48^{b}	12.74±0.84^{c}	
CH/CMCH	253.13±65.14^{b}	11.90±0.24^{a}		23.71±4.14^{ab}	10.51±0.53^{c}		451.83±56.92^{b}	11.23±0.59^{a}		25.23±3.76^{b}	8.74±0.79^{b}	
C1.2	622.00±40.62^{d}	14.13±0.17^{c}		15.90±2.79^{a}	5.60±0.41^{a}		820.63±45.59^{d}	15.23±0.09^{c}		15.68±2.62^{a}	5.27±0.90^{a}	
C1.8	690.60±12.34^{d}	14.10±0.33^{c}		18.88±6.06^{a}	4.61±0.49^{a}		814.20±16.26^{d}	13.43±0.05^{b}		20.32±4.41^{ab}	7.10±0.72^{ab}	
C2.4	410.27±26.26^{c}	12.90±0.16^{b}		21.43±0.98^{ab}	8.06±0.50^{b}		543.60±16.90^{c}	12.97±0.37^{b}		22.14±5.43^{ab}	8.65±1.54^{b}	

$^{\#}$C1.2 means CH/CMCH1.2; C1.8 means CH/CMCH1.8; C2.4 means CH/CMCH2.4.

*Different superscripts (a-d) within a column indicate significant differences among samples (p<0.05)

4. Conclusions

In the present study, the novel CMLLA was successfully developed and the improved antioxidant and antimicrobial properties of incorporated melatonin were presented. Among all prepared samples, the CMLLA system loading 1.2% CH，0.8% CMC，and 50mg/L MLT was potentially applied in fresh products. Incorporation of CMC and MLT greatly improved the mechanical strength (increased by 100%), opacity; while the water barrier property was enhanced. Structural characterization further verified the compatibility of the component polymers and improved properties were ascribed to the cross-linking interaction between CMC and chitosan. Besides, CMLLA was also shown antioxidant and antimicrobial activities. Moreover, results from the present study demonstrated the practical applicability of the developed CMLLA on fresh-cut cucumbers, broccolis and melons by maintaining the quality attributes including firmness, total soluble solid and chlorophyll contents; while preventing the weight loss and color degradation. Conclusively, the improvement of mechanical strength and morphological characteristics of CMLLA indicated that the chitosan incorporated with MLT and CMC was potentially applied in maintaining post-harvest quality of fresh products, although further research is essential to evaluate the safety of the CMLLA system before commercialization.

Reference

Aghdam, M. S., & Fard, J. R. (2017). Melatonin treatment attenuates postharvest decay and maintains nutritional quality of strawberry fruits (*Fragaria* × *anannasa cv. Selva*) by enhancing GABA shunt activity. *Food Chemistry*, *221*, 1650–1657. https://doi.org/10.1016/j.foodchem.2016.10.123

Aider, M. (2010). Chitosan application for active bio-based films production and potential in the food industry: Review. *LWT - Food Science and Technology*, *43*(6), 837–842. https://doi.org/10.1016/j.lwt.2010.01.021

Ali, A., Muhammad, M. T. M., Sijam, K., & Siddiqui, Y. (2011). Effect of chitosan coatings on the physicochemical characteristics of Eksotika II papaya (*Carica papaya L.)* fruit during cold storage. *Food Chemistry*, *124*(2), 620–626. https://doi.org/10.1016/j.foodchem.2010.06.085

Aljawish, A., Muniglia, L., Klouj, A., Jasniewski, J., Scher, J., & Desobry, S. (2016). Characterization of films based on enzymatically modified chitosan derivatives with phenol compounds. *Food Hydrocolloids*, *60*, 551–558. https://doi.org/10.1016/j.foodhyd.2016.04.032

Alvarez, M. V., Ponce, A. G., & Moreira, M. del R. (2013). Antimicrobial efficiency of chitosan coating enriched with bioactive compounds to improve the safety of fresh cut broccoli. *LWT - Food Science and Technology*, *50*(1), 78–87. https://doi.org/10.1016/j.lwt.2012.06.021

Arnao, M. B., & Hernández-Ruiz, J. (2017). Melatonin and its relationship to plant hormones. *Annals of Botany*, *121*(2), 195–207. https://doi.org/10.1093/aob/mcx114

Arnao, M., & Hernández-Ruiz, J. (2008). Protective effect of melatonin against chlorophyll degradation during the senescence of barley leaves. *Journal of Pineal Research*, *46*, 58–63. https://doi.org/10.1111/j.1600-079X.2008.00625.x

Bao, D., Chen, M., Wang, H., Wang, J., Liu, C., & Sun, R. (2014). Preparation and characterization of double crosslinked hydrogel films from carboxymethylchitosan and carboxymethylcellulose. *Carbohydrate Polymers*, *110*, 113–120. https://doi.org/10.1016/j.carbpol.2014.03.095

Blažević, F., Milekić, T., Romić, M. D., Juretić, M., Pepić, I., Filipović-Grčić, J., … Hafner, A. (2016). Nanoparticle-mediated interplay of chitosan and melatonin for improved wound epithelialisation. *Carbohydrate Polymers*, *146*, 445–454. https://doi.org/10.1016/j.carbpol.2016.03.074

Boy, R., Maness, C., & Kotek, R. (2015). Properties of Chitosan/Soy Protein Blended Films with Added Plasticizing Agent as a Function of Solvent Type at Acidic pH. *International Journal of Polymeric Materials and Polymeric Biomaterials*, *65*, 150923085124007. https://doi.org/10.1080/00914037.2015.1038821

Branca, C., D'Angelo, G., Crupi, C., Khouzami, K., Rifici, S., Ruello, G., & Wanderlingh, U. (2016). Role of the OH and NH vibrational groups in polysaccharide-nanocomposite interactions: A FTIR-ATR study on chitosan and chitosan/clay films. *Polymer*, *99*, 614–622. https://doi.org/10.1016/j.polymer.2016.07.086

Brink, I., Šipailienė, A., & Leskauskaitė, D. (2019). Antimicrobial properties of chitosan and whey protein films applied on fresh cut turkey pieces. *International Journal of Biological Macromolecules*, *130*, 810–817. https://doi.org/10.1016/j.ijbiomac.2019.03.021

Chao, Z., Yue, M., Xiaoyan, Z., & Dan, M. (2010). Development of Soybean Protein-Isolate Edible Films Incorporated with Beeswax, Span 20, and Glycerol. *Journal of Food Science*, *75*, C493-7. https://doi.org/10.1111/j.1750-3841.2010.01666.x

Chen, C., & Ho, C. (1995). Antioxidant Properties of Polyphenols Extracted from Green and Black Teas. *Journal of Food Lipids*, *2*(1), 35–46. https://doi.org/10.1111/j.1745-4522.1995.tb00028.x

Chen, W., Li, Y., Yang, S., Yue, L., Jiang, Q., & Xia, W. (2015). Synthesis and antioxidant properties of chitosan and carboxymethyl chitosan-stabilized selenium nanoparticles.

Carbohydrate Polymers, *132*, 574–581. https://doi.org/10.1016/j.carbpol.2015.06.064

Chen, X., Lee, C. M., & Park, H. (2003). O/W Emulsification for the Self-Aggregation and Nanoparticle Formation of Linoleic Acid Modified Chitosan in the Aqueous System. Journal of Agricultural and Food Chemistry, 51(10), 3135–3139. https://doi.org/10.1021/jf0208482

Chung, Y. C., & Chen, C. Y. (2008). Antibacterial characteristics and activity of acid-soluble chitosan. *Bioresource Technology*, *99*(8), 2806–2814. https://doi.org/10.1016/j.biortech.2007.06.044

de Abreu, F. R., & Campana-Filho, S. P. (2009). Characteristics and properties of carboxymethylchitosan. *Carbohydrate Polymers*, *75*(2), 214–221. https://doi.org/10.1016/j.carbpol.2008.06.009

de Moraes Crizel, T., de Oliveira Rios, A., D. Alves, V., Bandarra, N., Moldão-Martins, M., & Hickmann Flôres, S. (2018). Active food packaging prepared with chitosan and olive pomace. *Food Hydrocolloids*, *74*, 139–150. https://doi.org/10.1016/j.foodhyd.2017.08.007

Esteghlal, S., Niakousari, M., & Hosseini, S. M. H. (2018). Physical and mechanical properties of gelatin-CMC composite films under the influence of electrostatic interactions. *International Journal of Biological Macromolecules*, *114*, 1–9. https://doi.org/10.1016/j.ijbiomac.2018.03.079

Farshi Azhar, F., & Olad, A. (2014). A study on sustained release formulations for oral delivery of 5-fluorouracil based on alginate–chitosan/montmorillonite nanocomposite systems. *Applied Clay Science*, *101*, 288–296. https://doi.org/10.1016/j.clay.2014.09.004

Feng, F., Liu, Y., Zhao, B., & Hu, K. (2012). Characterization of half N-acetylated chitosan powders and films. *2011 Chinese Materials Conference*, *27*, 718–732. https://doi.org/10.1016/j.proeng.2011.12.511

Fernandez-Saiz, P., Lagaron, J. M., & Ocio, M. J. (2009). Optimization of the biocide properties of chitosan for its application in the design of active films of interest in the food area. *Food Hydrocolloids*, *23*(3), 913–921. https://doi.org/10.1016/j.foodhyd.2008.06.001

Fernández-Saiz, P., Sánchez, G., Soler, C., Lagaron, J. M., & Ocio, M. J. (2013). Chitosan films for the microbiological preservation of refrigerated sole and hake fillets. *Food Control*, *34*(1), 61–68. https://doi.org/10.1016/j.foodcont.2013.03.047

Gao, H., Zhang, Z. K., Chai, H. K., Cheng, N., Yang, Y., Wang, D. N., Cao, W. (2016). Melatonin treatment delays postharvest senescence and regulates reactive oxygen species metabolism in peach fruit. *Postharvest Biology and Technology*, *118*, 103–110. https://doi.org/10.1016/j.postharvbio.2016.03.006

Gennadios, A., Hanna, M. A., & Kurth, L. B. (1997). Application of Edible Coatings on Meats, Poultry and Seafoods: A Review. *LWT - Food Science and Technology*, *30*(4), 337–350. https://doi.org/10.1006/fstl.1996.0202

Ghasemzadeh, H., Mahboubi, A., Karimi, K., & Hassani, S. (2016). Full polysaccharide chitosan-CMC membrane and silver nanocomposite: Synthesis, characterization, and antibacterial behaviors. *Polymers for Advanced Technologies*, *27*, n/a-n/a. https://doi.org/10.1002/pat.3785

Guo, Z., Xing, R., Liu, S., Yu, H., Wang, P., Li, C., & Li, P. (2005). The synthesis and antioxidant activity of the Schiff bases of chitosan and carboxymethyl chitosan. *Bioorganic & Medicinal Chemistry Letters*, *15*(20), 4600–4603. https://doi.org/10.1016/j.bmcl.2005.06.095

Huang, Y., Wang, Y. J., Wang, Y., Yi, S., Fan, Z., Sun, L., Zhang, M. (2015). Exploring naturally occurring ivy nanoparticles as an alternative biomaterial. *Acta Biomaterialia*, *25*, 268–283. https://doi.org/10.1016/j.actbio.2015.07.035

Jeon, Y. (2001). Antimicrobial effect of chitooligosaccharides produced by bioreactor. *Carbohydrate Polymers*, *44*(1), 71–76. https://doi.org/10.1016/S0144-8617(00)00200-9

Kader, A. (2002). Quality Parameters of Fresh-cut Fruit and Vegetable Products. In *Fresh-Cut*

Fruits and Vegetables: Science, Technology, and Market. https://doi.org/10.1201/9781420031874.ch2

Kennedy, R., Costain, D. J., McAlister, V. C., & Lee, T. D. G. (1996). Prevention of experimental postoperative peritoneal adhesions by N,O-carboxymethyl chitosan. *Surgery*, *120*(5), 866–870. https://doi.org/10.1016/S0039-6060(96)80096-1

Kritchenkov, A. S., Egorov, A. R., Kurasova, M. N., Volkova, O. V., Meledina, T. V., Lipkan, N. A., dos Santos, W. M. (2019). Novel non-toxic high efficient antibacterial azido chitosan derivatives with potential application in food coatings. *Food Chemistry*, *301*, 125247. https://doi.org/10.1016/j.foodchem.2019.125247

Kucukgulmez, A., Celik, M., Yanar, Y., Sen, D., Polat, H., & Kadak, A. E. (2011). Physicochemical characterization of chitosan extracted from Metapenaeus stebbingi shells. *Food Chemistry*, *126*(3), 1144–1148. https://doi.org/10.1016/j.foodchem.2010.11.148

Kurek, M., Guinault, A., Voilley, A., Galić, K., & Debeaufort, F. (2014). Effect of relative humidity on carvacrol release and permeation properties of chitosan based films and coatings. *Special Issue: 7th International Conference on Water in Food*, *144*, 9–17. https://doi.org/10.1016/j.foodchem.2012.11.132

Lee, S., Han, J., & Han, J. (2015). Development and Evaluation of Apple Peel- and Carboxymethylcellulose-Based Biodegradable Films with Antioxidant and Antimicrobial Properties. *Journal of Food Safety*, *36*, n/a-n/a. https://doi.org/10.1111/jfs.12246

Li, F. X., Ma, B. X., He, Q. H., Lü, C., Wang, B., & Tian, H. (2013). Non-destructive Detection of Firmness of Hami Melon by Hyperspectral Imaging Technique. *Guangzi Xuebao/Acta Photonica Sinica*, *42*, 592–595. https://doi.org/10.3788/gzxb20134205.0592

Li, K., Zhu, J., Guan, G., & Wu, H. (2019). Preparation of chitosan-sodium alginate films through layer-by-layer assembly and ferulic acid crosslinking: Film properties, characterization, and formation mechanism. *International Journal of Biological Macromolecules*, *122*, 485–492. https://doi.org/10.1016/j.ijbiomac.2018.10.188

Lin, L., Xue, L., Duraiarasan, S., & Haiying, C. (2018). Preparation of ε-polylysine/chitosan nanofibers for food packaging against Salmonella on chicken. *Food Packaging and Shelf Life*, *17*, 134–141. https://doi.org/10.1016/j.fpsl.2018.06.013

Liu, C., Zheng, H., Sheng, K., Liu, W., & Zheng, L. (2018). Effects of melatonin treatment on the postharvest quality of strawberry fruit. *Postharvest Biology and Technology*, *139*, 47–55. https://doi.org/10.1016/j.postharvbio.2018.01.016

Liu, Jianlong, Zhang, R., Sun, Y., Liu, Z., Jin, W., & Sun, Y. (2016). The beneficial effects of exogenous melatonin on tomato fruit properties. *Scientia Horticulturae*, *207*, 14–20. https://doi.org/10.1016/j.scienta.2016.05.003

Liu, Jun, Liu, S., Chen, Y., Zhang, L., Kan, J., & Jin, C. (2017). Physical, mechanical and antioxidant properties of chitosan films grafted with different hydroxybenzoic acids. *Food Hydrocolloids*, *71*, 176–186. https://doi.org/10.1016/j.foodhyd.2017.05.019

Liu, Jun, Meng, C., Liu, S., Kan, J., & Jin, C. (2017). Preparation and characterization of protocatechuic acid grafted chitosan films with antioxidant activity. *Food Hydrocolloids*, *63*, 457–466. https://doi.org/10.1016/j.foodhyd.2016.09.035

Liu, Y., Cai, Y., Jiang, X., Wu, J., & Le, X. (2016). Molecular interactions, characterization and antimicrobial activity of curcumin–chitosan blend films. *Food Hydrocolloids*, *52*, 564–572. https://doi.org/10.1016/j.foodhyd.2015.08.005

Ma, Q., Zhang, T., Zhang, P., & Wang, Z. (2016). Melatonin attenuates postharvest physiological deterioration of cassava storage roots. *Journal of Pineal Research*, *60*, n/a-n/a. https://doi.org/10.1111/jpi.12325

Malafaya, P. B., Silva, G. A., & Reis, R. L. (2007). Natural–origin polymers as carriers and scaffolds for biomolecules and cell delivery in tissue engineering applications. *Advanced Drug Delivery Reviews*, *59*(4–5), 207–233. https://doi.org/10.1016/j.addr.2007.03.012

Martins, J. T., Cerqueira, M. A., & Vicente, A. A. (2012). Influence of α-tocopherol on physicochemical properties of chitosan-based films. *Food Hydrocolloids*, *27*(1), 220–227. https://doi.org/10.1016/j.foodhyd.2011.06.011

Mathew, S., & Abraham, T. E. (2008). Characterisation of ferulic acid incorporated starch–chitosan blend films. *Food Hydrocolloids*, *22*(5), 826–835. https://doi.org/10.1016/j.foodhyd.2007.03.012

Matinfar, M., Mesgar, A. S., & Mohammadi, Z. (2019). Evaluation of physicochemical, mechanical and biological properties of chitosan/carboxymethyl cellulose reinforced with multiphasic calcium phosphate whisker-like fibers for bone tissue engineering. *Materials Science and Engineering: C*, *100*, 341–353. https://doi.org/10.1016/j.msec.2019.03.015

Mayachiew, P., & Devahastin, S. (2010). Effects of drying methods and conditions on release characteristics of edible chitosan films enriched with Indian gooseberry extract. *Food Chemistry*, *118*(3), 594–601. https://doi.org/10.1016/j.foodchem.2009.05.027

Meng, J. F., Xu, T. F., Wang, Z., Fang, Y., Xi, Z., & Zhang, Z. (2014). The ameliorative effects of exogenous melatonin on grape cuttings under water-deficient stress: Antioxidant metabolites, leaf anatomy, and chloroplast morphology. *Journal of Pineal Research*, *57*. https://doi.org/10.1111/jpi.12159

Noronha, C. M., de Carvalho, S. M., Lino, R. C., & Barreto, P. L. M. (2014). Characterization of antioxidant methylcellulose film incorporated with α-tocopherol nanocapsules. *Food Chemistry*, *159*, 529–535. https://doi.org/10.1016/j.foodchem.2014.02.159

Ochoa-Velasco, C. E., & Guerrero-Beltrán, J. Á. (2014). Postharvest quality of peeled prickly pear fruit treated with acetic acid and chitosan. *Postharvest Biology and Technology*, *92*, 139–145. https://doi.org/10.1016/j.postharvbio.2014.01.023

Ohlemiller, K. K., & Frisina, R. D. (2008). Age-Related Hearing Loss and Its Cellular and Molecular Bases. In J. Schacht, A. N. Popper, & R. R. Fay (Eds.), *Auditory Trauma, Protection, and Repair* (pp. 145–194). https://doi.org/10.1007/978-0-387-72561-1_6

Okuyama, K., Noguchi, K., Kanenari, M., Egawa, T., Osawa, K., & Ogawa, K. (2000). Structural diversity of chitosan and its complexes. *Carbohydrate Polymers*, *41*(3), 237–247. https://doi.org/10.1016/S0144-8617(99)00142-3

Ortiz, A., Graell, J., & Lara, I. (2011). Preharvest calcium applications inhibit some cell wall-modifying enzyme activities and delay cell wall disassembly at commercial harvest of 'Fuji Kiku-8′ apples. *Postharvest Biology and Technology*, *62*(2), 161–167. https://doi.org/10.1016/j.postharvbio.2011.04.014

Park, H., Choi, B., Hu, J., & Lee, M. (2013). Injectable chitosan hyaluronic acid hydrogels for cartilage tissue engineering. *Acta Biomaterialia*, *9*(1), 4779–4786. https://doi.org/10.1016/j.actbio.2012.08.033

Portes, E., Gardrat, C., Castellan, A., & Coma, V. (2009). Environmentally friendly films based on chitosan and tetrahydrocurcuminoid derivatives exhibiting antibacterial and antioxidative properties. *Carbohydrate Polymers*, *76*(4), 578–584. https://doi.org/10.1016/j.carbpol.2008.11.031

Poverenov, E., Arnon-Rips, H., Zaitsev, Y., Bar, V., Danay, O., Horev, B., Rodov, V. (2018). Potential of chitosan from mushroom waste to enhance quality and storability of fresh-cut melons. *Food Chemistry*, *268*, 233–241. https://doi.org/10.1016/j.foodchem.2018.06.045

Qiu, L., Shao, Z., Wang, D., Wang, F., Wang, W., & Wang, J. (2014). Carboxymethyl cellulose lithium (CMC-Li) as a novel binder and its electrochemical performance in lithium-ion batteries. *Cellulose*, *21*, 2789–2796. https://doi.org/10.1007/s10570-014-0274-7

Rivero, S., García, M. A., & Pinotti, A. (2010). Crosslinking capacity of tannic acid in plasticized chitosan films. *Carbohydrate Polymers*, *82*(2), 270–276. https://doi.org/10.1016/j.carbpol.2010.04.048

Romić, M. D., Klarić, M. Š., Lovrić, J., Pepić, I., Cetina-Čižmek, B., Filipović-Grčić, J., & Hafner, A. (2016). Melatonin-loaded chitosan/Pluronic® F127 microspheres as in situ forming hydrogel: An innovative antimicrobial wound dressing. *European Journal of*

Pharmaceutics and Biopharmaceutics, *107*, 67–79. https://doi.org/10.1016/j.ejpb.2016.06.013

Rubilar, J. F., Cruz, R. M. S., Silva, H. D., Vicente, A. A., Khmelinskii, I., & Vieira, M. C. (2013). Physico-mechanical properties of chitosan films with carvacrol and grape seed extract. *2nd ISEKI_Food Conference*, *115*(4), 466–474. https://doi.org/10.1016/j.jfoodeng.2012.07.009

Sakurai, K. (2000). Glass transition temperature of chitosan and miscibility of chitosan/poly(*N-vinyl pyrrolidone*) blends. *Polymer*, *41*(19), 7051–7056. https://doi.org/10.1016/S0032-3861(00)00067-7

Sánchez-González, L., González-Martínez, C., Chiralt, A., & Cháfer, M. (2010). Physical and antimicrobial properties of chitosan–tea tree essential oil composite films. *Journal of Food Engineering*, *98*(4), 443–452. https://doi.org/10.1016/j.jfoodeng.2010.01.026

Sathivel, S. (2005). Chitosan and Protein Coatings Affect Yield, Moisture Loss, and Lipid Oxidation of Pink Salmon (Oncorhynchus gorbuscha) Fillets During Frozen Storage. *Journal of Food Science*, *70*, e455–e459. https://doi.org/10.1111/j.1365-2621.2005.tb11514.x

Sayari, N., Sila, A., Abdelmalek, B. E., Abdallah, R. B., Ellouz-Chaabouni, S., Bougatef, A., & Balti, R. (2016). Chitin and chitosan from the Norway lobster by-products: Antimicrobial and anti-proliferative activities. *International Journal of Biological Macromolecules*, *87*, 163–171. https://doi.org/10.1016/j.ijbiomac.2016.02.057

Seo, S., King, J. M., & Prinyawiwatkul, W. (2007). Simultaneous Depolymerization and Decolorization of Chitosan by Ozone Treatment. *Journal of Food Science*, *72*(9), C522–C526. https://doi.org/10.1111/j.1750-3841.2007.00563.x

Seydim, A. C., & Sarikus, G. (2006). Antimicrobial activity of whey protein based edible films incorporated with oregano, rosemary and garlic essential oils. *Food Research International*, *39*(5), 639–644. https://doi.org/10.1016/j.foodres.2006.01.013

Shi, H., Chen, Y., Tan, D. X., Reiter, R., Chan, Z., & He, C. (2015). Melatonin induces nitric oxide and the potential mechanisms relate to innate immunity against bacterial pathogen infection in Arabidopsis. *Journal of Pineal Research*, *59*, 102–108. https://doi.org/10.1111/jpi.12244

Shi, H., Reiter, R., Tan, D. X., & Chan, Z. (2014). Indole-3-acetic Acid Inducible 17 positively modulates natural leaf senescence through melatonin-mediated pathway in Arabidopsis. *Journal of Pineal Research*, *58*, 26–33. https://doi.org/10.1111/jpi.12188

Siripatrawan, U., & Harte, B. R. (2010). Physical properties and antioxidant activity of an active film from chitosan incorporated with green tea extract. *Food Hydrocolloids*, *24*(8), 770–775. https://doi.org/10.1016/j.foodhyd.2010.04.003

Sogut, E., & Seydim, A. C. (2018). Development of Chitosan and Polycaprolactone based active bilayer films enhanced with nanocellulose and grape seed extract. *Carbohydrate Polymers*, *195*, 180–188. https://doi.org/10.1016/j.carbpol.2018.04.071

Song, R., Murphy, M., Li, C., Ting, K., Soo, C., & Zheng, Z. (2018). Current development of biodegradable polymeric materials for biomedical applications. *Drug Design, Development and Therapy*, *12*, 3117–3145. https://doi.org/10.2147/DDDT.S165440

Soultos, N., Tzikas, Z., Abrahim, A., Georgantelis, D., & Ambrosiadis, I. (2008). Chitosan effects on quality properties of Greek style fresh pork sausages. *Meat Science*, *80*(4), 1150–1156. https://doi.org/10.1016/j.meatsci.2008.05.008

Sozer, N., & Kokini, J. L. (2009). Nanotechnology and its applications in the food sector. *Trends in Biotechnology*, *27*(2), 82–89. https://doi.org/10.1016/j.tibtech.2008.10.010

Su, J. F., Huang, Z., Yuan, X. Y., Wang, X. Y., & Li, M. (2010). Structure and properties of carboxymethyl cellulose/soy protein isolate blend edible films crosslinked by Maillard reactions. *Carbohydrate Polymers*, *79*(1), 145–153. https://doi.org/10.1016/j.carbpol.2009.07.035

Sun, L., Sun, J., Chen, L., Niu, P., Yang, X., & Guo, Y. (2017). Preparation and characterization

of chitosan film incorporated with thinned young apple polyphenols as an active packaging material. *Carbohydrate Polymers*, *163*, 81–91. https://doi.org/10.1016/j.carbpol.2017.01.016

Sun, Y., Liu, Z., Lan, G., Jiao, C., & Sun, Y. (2019). Effect of exogenous melatonin on resistance of cucumber to downy mildew. *Scientia Horticulturae*, *255*, 231–241. https://doi.org/10.1016/j.scienta.2019.04.057

Takeda, Y., Yoza, K. I., Nogata, Y., & Ohta, H. (1993). Effects of Storage Temperatures on Polyamine Content of Some Leafy Vegetables. *Journal of the Japanese Society for Horticultural Science*, *62*(2), 425–430. https://doi.org/10.2503/jjshs.62.425

Tan, D. X., Manchester, L. C., Helton, P., & Reiter, R. J. (2007). Phytoremediative capacity of plants enriched with melatonin. *Plant Signaling & Behavior*, *2*(6), 514–516. https://doi.org/10.4161/psb.2.6.4639

Tan, Y. M., Lim, S. H., Tay, B. Y., Lee, M. W., & Thian, E. S. (2015). Functional chitosan-based grapefruit seed extract composite films for applications in food packaging technology. *SI: 6th ISFM 2014*, *69*, 142–146. https://doi.org/10.1016/j.materresbull.2014.11.041

Tang, X. Z., Kumar, P., Alavi, S., & Sandeep, K. P. (2012). Recent Advances in Biopolymers and Biopolymer-Based Nanocomposites for Food Packaging Materials. *Critical Reviews in Food Science and Nutrition*, *52*(5), 426–442. https://doi.org/10.1080/10408398.2010.500508

Tang, Y., Yang, X., Hang, B., Li, J., Huang, L., Huang, F., & Xu, Z. (2016). Efficient Production of Hydroxylated Human-Like Collagen Via the Co-Expression of Three Key Genes in *Escherichia coli Origami* (DE3). *Applied Biochemistry and Biotechnology*, *178*(7), 1458–1470. https://doi.org/10.1007/s12010-015-1959-6

Tekbas, O. F., Ogur, R., Korkmaz, A., Kilic, A., & Reiter, R. J. (2008). Melatonin as an antibiotic: New insights into the actions of this ubiquitous molecule. *Journal of Pineal Research*, *44*(2), 222–226. https://doi.org/10.1111/j.1600-079X.2007.00516.x

US FDA (US Food and Drug Administration). Center for Food Safety and Applied Nutrition. Office of Premarket Approval. *GRAS notices received in 2001. Available at: <http:/vm.cfsan.fda.gov>.*

Van den Broek, L. A. M., Knoop, R. J. I., Kappen, F. H. J., & Boeriu, C. G. (2015). Chitosan films and blends for packaging material. *Carbohydrate Polymers*, *116*, 237–242. https://doi.org/10.1016/j.carbpol.2014.07.039

Vielma, J. R., Bonilla, E., Chacín Bonilla, L., Mora, M., Medina Leendertz, S., & Bravo, Y. (2014). Effects of melatonin on oxidative stress, and resistance to bacterial, parasitic, and viral infections: A review. *Acta Tropica*, *137*, 31–38. https://doi.org/10.1016/j.actatropica.2014.04.021

Wahid, F., Yin, J. J., Xue, D. D., Xue, H., Lu, Y. S., Zhong, C., & Chu, L. Q. (2016). Synthesis and characterization of antibacterial carboxymethyl Chitosan/ZnO nanocomposite hydrogels. *International Journal of Biological Macromolecules*, *88*, 273–279. https://doi.org/10.1016/j.ijbiomac.2016.03.044

Wang, H., Gong, X., Miao, Y., Guo, X., Liu, C., Fan, Y. Y., Li, W. (2019). Preparation and characterization of multilayer films composed of chitosan, sodium alginate and carboxymethyl chitosan-ZnO nanoparticles. *Food Chemistry*, *283*, 397–403. https://doi.org/10.1016/j.foodchem.2019.01.022

Wang, K., Lim, P. N., Tong, S. Y., & Thian, E. S. (2019). Development of grapefruit seed extract-loaded poly(*ε-caprolactone*)/chitosan films for antimicrobial food packaging. *Food Packaging and Shelf Life*, *22*, 100396. https://doi.org/10.1016/j.fpsl.2019.100396

Wang, S. F., Shen, L., Tong, Y. J., Chen, L., Phang, I. Y., Lim, P. Q., & Liu, T. X. (2005). Biopolymer chitosan/montmorillonite nanocomposites: Preparation and characterization. *Polymer Degradation and Stability*, *90*(1), 123–131. https://doi.org/10.1016/j.polymdegradstab.2005.03.001

Wang, X., Yong, H., Gao, L., Li, L., Jin, M., & Liu, J. (2019). Preparation and characterization of

antioxidant and pH-sensitive films based on chitosan and black soybean seed coat extract. *Food Hydrocolloids*, *89*, 56–66. https://doi.org/10.1016/j.foodhyd.2018.10.019

Wang, Y., Reiter, R., & Chan, Z. (2017). Phytomelatonin: A universal abiotic stress regulator. *Journal of Experimental Botany*, *69*. https://doi.org/10.1093/jxb/erx473

Wu, C., Tian, J., Li, S., Wu, T., Hu, Y., Chen, S., Ye, X. (2016). Structural properties of films and rheology of film-forming solutions of chitosan gallate for food packaging. *Carbohydrate Polymers*, *146*, 10–19. https://doi.org/10.1016/j.carbpol.2016.03.027

Xin, D., Si, J., & Kou, L. (2017). Postharvest exogenous melatonin enhances quality and delays the senescence of cucumber. *Acta Horticulturae Sinica*, *44*, 891–901. https://doi.org/10.16420/j.issn.0513-353x.2016-0888

Yan, J., Luo, Z., Ban, Z., Lu, H., Li, D., Yang, D., … Li, L. (2019). The effect of the layer-by-layer (LBL) edible coating on strawberry quality and metabolites during storage. *Postharvest Biology and Technology*, *147*, 29–38. https://doi.org/10.1016/j.postharvbio.2018.09.002

Yang, H., Yan, R., Chen, H., Lee, D. H., & Zheng, C. (2007). Characteristics of hemicellulose, cellulose and lignin pyrolysis. *Fuel*, *86*(12), 1781–1788. https://doi.org/10.1016/j.fuel.2006.12.013

Yen, M. T., Yang, J. H., & Mau, J. L. (2008). Antioxidant properties of chitosan from crab shells. *Carbohydrate Polymers*, *74*(4), 840–844. https://doi.org/10.1016/j.carbpol.2008.05.003

Yu, S. H., Hsieh, H. Y., Pang, J. C., Tang, D. W., Shih, C. M., Tsai, M. L., Mi, F. L. (2013). Active films from water-soluble chitosan/cellulose composites incorporating releasable caffeic acid for inhibition of lipid oxidation in fish oil emulsions. *Food Hydrocolloids*, *32*(1), 9–19. https://doi.org/10.1016/j.foodhyd.2012.11.036

Zhai, L., Bai, Z., Zhu, Y., Wang, B., & Luo, W. (2018). Fabrication of chitosan microspheres for efficient adsorption of methyl orange. *Chinese Journal of Chemical Engineering*, *26*(3), 657–666. https://doi.org/10.1016/j.cjche.2017.08.015

Zhang, J., Shi, Y., Zhang, X., Du, H., Xu, B., & Huang, B. (2017). Melatonin suppression of heat-induced leaf senescence involves changes in abscisic acid and cytokinin biosynthesis and signaling pathways in perennial ryegrass (*Lolium perenne L.*). *Environmental and Experimental Botany*, *138*, 36–45. https://doi.org/10.1016/j.envexpbot.2017.02.012

Zhao, D., Huang, J., Hu, S., Mao, J., & Mei, L. (2011). Biochemical activities of N,O-carboxymethyl chitosan from squid cartilage. *Carbohydrate Polymers*, *85*(4), 832–837. https://doi.org/10.1016/j.carbpol.2011.04.007

Zhao, Q., Qian, J., An, Q., Gao, C., Gui, Z., & Jin, H. (2009). Synthesis and characterization of soluble chitosan/sodium carboxymethyl cellulose polyelectrolyte complexes and the pervaporation dehydration of their homogeneous membranes. *Journal of Membrane Science*, *333*(1), 68–78. https://doi.org/10.1016/j.memsci.2009.02.001

Zhuang, C., Jiang, Y., Zhong, Y., Zhao, Y., Deng, Y., Yue, J., Mu, H. (2018). Development and characterization of nano-bilayer films composed of polyvinyl alcohol, chitosan and alginate. *Food Control*, *86*, 191–199. https://doi.org/10.1016/j.foodcont.2017.11.024